Surface Chemical Composition Analysis in Polystyrene/Poly(vinyl methyl ether) Blend Films by UV Reflection Spectroscopy

Sangmook Lee and Chong Sook P. Sung*

Polymer Program, Department of Chemistry, Institute of Materials Science, 97 North Eagleville Rd., University of Connecticut, Storrs, Connecticut 06269-3136

Received April 11, 2000; Revised Manuscript Received September 12, 2000

ABSTRACT: Surface chemical composition in miscible polymer blend films was measured by UV reflection spectroscopy, using polystyrene (PS) as chromophores in blends with poly(vinyl methyl ether) (PVME). Kramers−Kronig transformation from UV reflection spectra was performed to obtain the optical constant (k) spectra, from which the surface composition of PS in blend films was estimated. The results show surface excess of PVME in a range of bulk blend compositions when M_w of PS and PVME was 240 000 and 99 000, respectively. This surface composition probes the surface depth of several hundreds of angstroms, which is deeper than the probed depth of ESCA but shallower than that of IR-ATR. In miscible PS/PVME blends, the experimentally obtained surface composition facing air compares well with the prediction from the simplified mean-field theory of Jones and Kramer but shows less PVME enrichment than the results by ESCA. For the in-situ technique, UV reflection via bifurcated fiber-optic accessory was found to provide similar results as the reflection accessory. Also, the polymer−quartz interface and heat treatment effects were investigated. The polymer−quartz interface showed less enrichment of PVME than the air-facing surface, while the blend surface facing air was more enriched in PVME after thermal treatment.

Introduction

Surface chemical composition in polymer blends is known to be affected by various factors such as the blend composition,[1] film thickness,[2,3] molecular weight,[1,4,5] and the substrate[6] on which the film is cast. Various techniques such as ESCA,[1,4,7] IR-ATR,[6,8,9] surface-enhanced Raman,[5] SIMS,[4,7,10] and neutron reflection[11] have been used for the measurement of surface chemical composition, while atomic force microscopy (AFM)[2−4,7] and fluorescence confocal microscopy[12] have been used for surface morphology characterization.

Depending on the factors described above, the results indicated that the surface chemical composition in polymer blends is often different from that of the bulk. The general trend is such that the lower surface energy component tends to migrate toward the air-facing surface.

Various experimental techniques probe different surface depths. Some techniques such as ESCA and SIMS probe in the tens of angstroms range of the surface, while IR-ATR probes usually in the micron range. It would be very useful to have an experimental technique to probe in the hundreds of angstroms range of the surface. For example, many nanomaterials have thickness in this range. In principle, UV external reflection based on intrinsic chromophores in solid films can probe in this intermediate range depending on the chromophores concentration, c (mol/L), and its extinction coefficient.[13,14]

According to Kaito et al.,[13,14] the probed depth (d_p) by UV reflection is expressed in eq 1,

$$d_p = \frac{\lambda}{4\pi k} = \frac{1}{\epsilon c \ln 10} = \frac{10^{-3} M}{\epsilon \rho \ln 10} \qquad (1)$$

In eq 1, M is the molecular weight of the repeating chromophore unit, ρ is the density (g/cm^3), ϵ is the molar extinction coefficient, and k is the absorption index. When using intrinsic UV reflection from aromatic chromophores, the extinction coefficient, ϵ is on the order of 10^4 L/(mol cm). Therefore, d_p is on the order of 100−1000 Å. In this work, the depth of penetration for PS is estimated to be ∼200 Å, which is close to the experimental value of 250−450 Å at about 197 nm as will be described in a later section. In addition to this depth range, which is not readily available by other techniques, the UV reflection technique can be implemented as a nondestructive, in-situ, in-process analytical technique to continuously monitor surface chemical composition via bifurcated fiber-optic accessory.[16] In this paper, we report on UV reflection technique by using both reflection accessory and fiber-optic accessory to investigate PS/PVME blends. The experimental results on miscible blend will be compared with the predictions from a simplified theory[17] based on mean-field theory.

Experimental Section

Materials and Film Preparation. The polystyrene (M_w of 240 000 with polydispersity of 2.01) and the poly(vinyl methyl ether) (M_w of 99 000) purchased from Scientific Polymer Product Inc. were used as obtained. A series of PS/PVME blends were investigated. For surface composition analyses, 10 wt % solutions of the blends in UV grade toluene were used to cast blend films. Another series of PS solutions with lower concentration (0.03−4 wt %) were prepared to estimate the depth of penetration.

Synthetic fused silicon disks were washed several times with UV grade toluene and dried in an oven at 150 °C for 2 h, before casting films on them, and dried gradually in the hood and under vacuum at 60 °C at least 4 days to remove toluene. The films were found to have thickness of 30−50 mm, based on the transmission UV absorbance spectra. No evidence of residual toluene was found in the UV-reflection spectra of PVME films, after this drying process. The same drying conditions were applied for the depth of penetration studies.

UV Reflectance Measurements. UV reflection spectra were obtained with a Perkin-Elmer Lambda 6 UV spectrometer using an external reflection accessory as in Figure 1a,

10.1021/ma000633y CCC: $20.00
Published on Web 12/23/2000

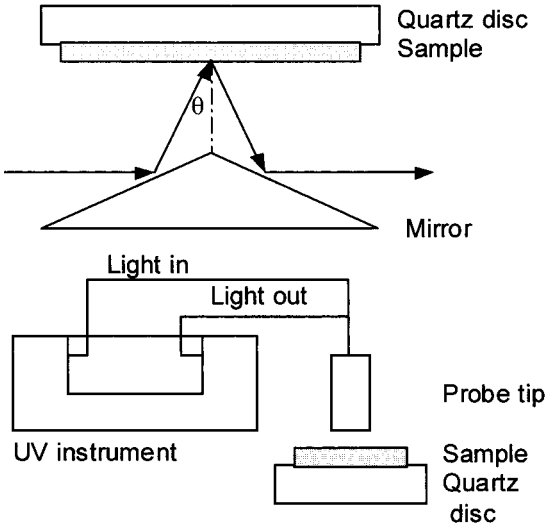

Figure 1. Schematic diagram showing (a, top) optical pathway of specular reflection on polymer sample and (b, bottom) UV reflection setup with a bifurcated fiber-optic attachment.

where the incident and the reflection angles were at 6° from the vertical position. To develop in-situ composition analysis technique, a bifurcated fiber-optic probe[16,18] was used as illustrated in Figure 1b. In this probe, both the core and cladding consist of UV grade fused silica. The UV source and the detector side have 70 hexagonally packed fibers, while the probe tip consists of a random mix of 140 hexagonally packed fibers. The distance between fiber tip and the film was 1.7 mm, which is found to be the optimum condition.[16,18] The beam size for this setup is about 7 mm^2, large enough to average the samples.

ESCA Measurements. ESCA spectra were obtained with a modified AEI ES200B spectrometer by using Al Kα exciting radiation source ($h\nu$ = 1486.7 eV), under the operating condition of 10 kV and 60 mA with the pressure in the source chamber at (2−4) × 10^{-8} Torr. Both PS and PVME contain hydrogen carbon, and therefore the binding energy of the C_{1S} signal at 285.0 eV (hydrogen carbon) was used as an internal calibration standard of the absolute binding energy scale. ESCA measurements were obtained at a fixed takeoff angle of 60°.

Results and Discussion

Peak Assignments and Depth of Penetration. A typical UV absorption spectrum and reflection spectrum of PS are shown in Figure 2. The PS spectrum has three peaks in the range 190−280 nm. According to Partridge,[19] the first, very strong peak at about 194 nm with an extinction coefficient of 24 500 L/(mol cm)[18] is analogous to the allowed benzene transition at about 179 nm. The next peak shown by shoulder near 215 nm is analogous to the forbidden benzene transition at about 200 nm. The third peak around 260 nm which is much weaker than the first two peaks is clearly analogous to the forbidden benzene transition in 260 nm region. In this work, we used the strongest peak at about 194 nm to represent surface composition of PS, because the second peak is obscured by a scattering peak at 240 nm[18,19] and the third peak is too weak for accurate measurement.

To estimate the probed depth by UV reflection technique, thin PS films with various thickness were prepared. Their thickness calculated from the transmission absorbance using Beer's law with the extinction coefficient at 197 nm of 24 500 L/(mol cm) for solid film[19] and c of 10.096 mol/L was in the range 21−1150 Å. The reflectance at 197 nm increased with film thickness up

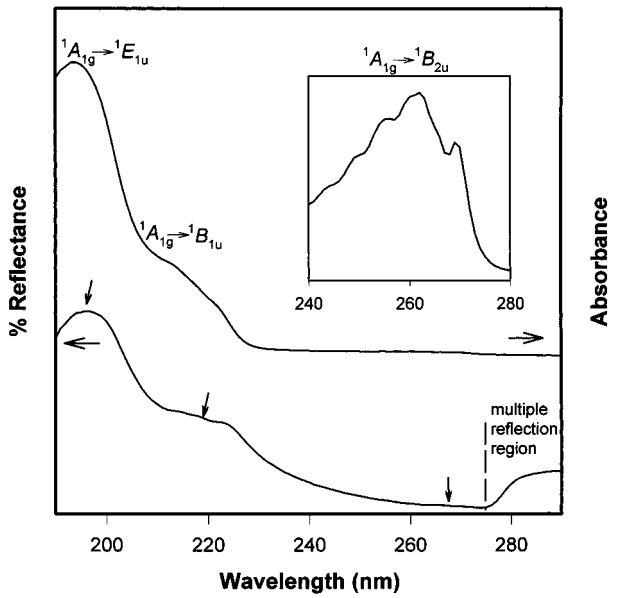

Figure 2. Absorption and reflection spectra of polystyrene film coated on quartz disk.

to 250−450 Å, but beyond this range, it stayed constant. Thus, we may conclude that the probed depth is 250−450 Å. On the other hand, the depth of penetration was calculated with ϵ for solid film[19] using eq 1 was about 180 Å. In blend films, the penetration depth will be deeper since the pure PS layer is not expected on the surface.

Experimental Results in PS/PVME Blends at Equilibrium. The percent reflectance, R, from UV reflection spectra is not proportional to the concentration of chromophore but is function of only two parameters, i.e., for pure PS, the refractive index and absorption index k. It would be necessary to obtain an absorption index k, which is proportional to the concentration of chromophore, as shown in eq 2.[21]

$$c = \frac{4\pi k}{\ln 10 \lambda \epsilon} \tag{2}$$

where λ and ϵ are the wavelength of light and extinction coefficient, respectively.

The reflection spectra is shifted from that of transmission spectra by a phase shift ϕ. The absorption index, k, is related to R and ϕ for normal incidence angle,[22] as in eq 3.

$$k = \frac{-2\sqrt{R}\sin\phi}{1 + R - 2\sqrt{R}\cos\phi} \tag{3}$$

Therefore, k can be obtained by measuring R and by calculating ϕ through the following Kramers−Kronig dispersion equation:[23]

$$\phi(\omega_0) = -\frac{\omega_0}{\pi}\int_0^\infty \frac{\ln R(\omega) - \ln R(\omega_0)}{\omega^2 - \omega_0^2}\,d\omega \tag{4}$$

where ω_0 is a particular wavenumber. Equation 4 shows that the phase shift, ϕ, at ω_0 can be calculated from the dispersion of reflectance by integrating from zero to infinite frequencies. However, only a limited region of the whole spectral range makes a significant contribution to $\phi(\omega_0)$. The major contributions came from the neighborhood of ω_0 (near the singular point) since the

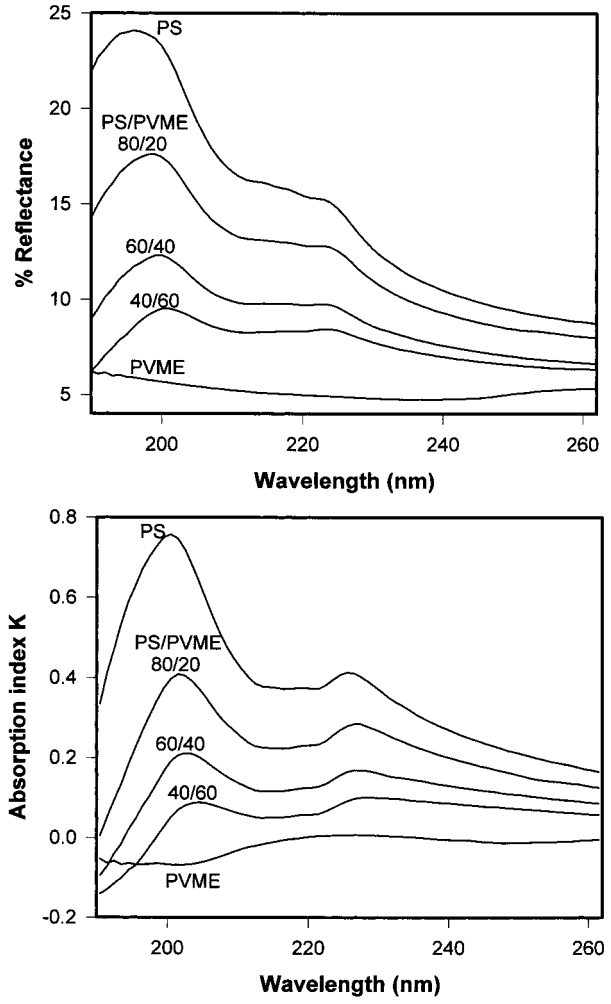

Figure 3. PS/PVME results: (a, top) UV reflection spectra and (b, bottom) absorption index *k* spectra.

function $1/(\omega^2 - \omega_0^2)$ is strongly peaked when ω approaches ω_0. Thus, only part of the spectrum representing the absorption band is required to calculate $\phi(\omega_0)$. Equation 4 can be calculated by a fast Fourier transform algorithm on a personal computer as described by Bortz and French,[24] other numerical methods,[25] or commercially available software.[26] However, in this work, to avoid the singular point and to increase the accuracy of the integration, we adopted a central difference technique based on finite difference method,[27,28] using eq 5

$$\phi(\omega_0)_{i+0.5} = -\frac{\omega_{0i+0.5}}{\pi}\sum_{i=a}^{b}\frac{\ln R(\omega)_i - \ln R(\omega_0)_{i+0.5}}{\omega_i^2 - \omega_0^2{}_{i+0.5}}\Delta\omega \tag{5}$$

where *a* is the lower wavelength range and *b* is the upper wavelength range.

The method proposed by Roessler has been used in UV reflectance spectral analysis of poly(ethylene terephthalate) to evaluate the contribution to the phase shift from the reflectance outside the experimental region. However, Roessler's method requires the spectra to have two zero values of *k* in the spectra, which is not the case for the 200 nm peak in polystyrene.

Figure 3a shows UV reflection spectra of PS/PVME blends. The lack of UV peak around 200 nm in PVME film supports that toluene is dried off under the drying

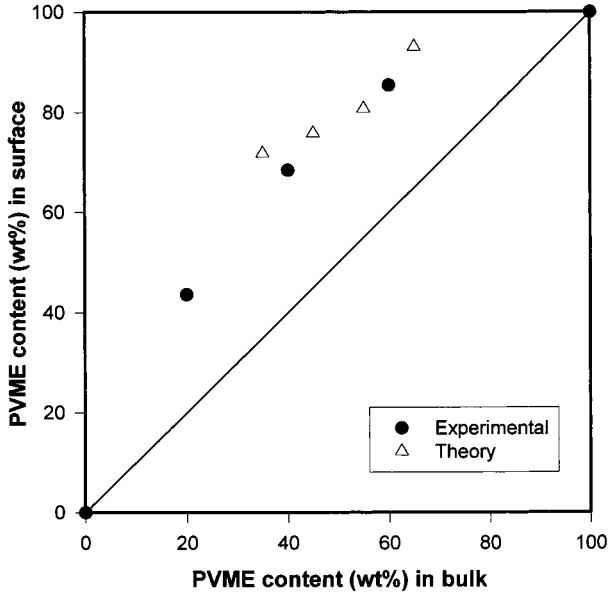

Figure 4. Comparison of PS/PVME results with simplified mean-field theory.

conditions. For PVME films studied, no multiple reflection is observed in the spectral range investigated. To retrieve the concentration of PS from the reflection spectra, Kramers−Kronig conversion was obtained as illustrated in Figure 3b, by using eq 5. Several observations can be made in Figure 3b. First, the transformed spectra as shown in Figure 3b are red-shifted to some extent in comparison to the reflection spectra of Figure 3a, an expected trend as observed in many cases.[13,15b] Second, for some blends such as 40/60 and PVME, negative values of *k* are obtained at shorter wavelengths due to the limitation of eq 5. This trend is due to the fact that only limited region was integrated. However, when the blend composition is calculated, we use PVME spectra at 200 nm in Figure 3b as a baseline to compensate for the negative value. Another observation from Figure 3b is the appearance of the second peak near 225 nm, which is red-shifted from the second absorption at 215 nm. In the reflection spectra, scattering near 240 nm makes a contribution to the peak near 225 nm. Therefore, this second peak is not accurate even after Kramers−Kronig conversion. The same trend is found for the third peak near 260 nm, which is supposed to be much weaker than the second peak, but shows *k* values of 0.2−0.3, as observed by Carter et al.[19] As pointed out by Patridge,[18] the third peak's accuracy is poor in reflection spectra, probably due to contributions from 240 nm scattering and multiple reflection. However, Patridge observed that the *k* value of the first peak is quite accurate, in comparison to the expected value from UV absorption spectra of thin polystyrene film. Therefore, we used the *k* values at around 200 nm in Figure 3b to represent PS content, k_{blend} in the blend, using PVME spectra at 200 nm as the baseline. The apparent surface composition of PVME (C_s) in blends is calculated by eq 6.

$$C_s = \frac{k_{PS} - k_{blend}}{k_{PS}} \tag{6}$$

where k_{PS} corresponds to the *k* value of pure PS, measured from PVME spectra near 200 nm. The resultant PVME surface contents are illustrated in Figure 4

as filled circles. Figure 4 shows that in toluene cast films of PS/PVME which are known to be miscible,[29] there is enrichment of PVME on the surface in comparison to bulk for all blend compositions studied. This finding is probably due to the migration of PVME; the lower surface energy component to the air-facing surface is consistent with the previously reported trend by ESCA[1] and IR-ATR.[6,8]

Comparison with Theory in PS/PVME Blends. In miscible polymer blend films which are at equilibrium, the simplified theory of Jones and Kramer[17] relates the surface volume composition (C_s) of the lower surface energy component to the bulk volume composition (C_b) by eq 7.

$$C_s = \frac{C_b + t}{1 + t} \tag{7}$$

The parameter t depends on the difference in surface energies ($\Delta\gamma$) between the two polymers and the interaction parameter χ between the segments of the two polymers and takes the form expressed in eq 8.

$$t = \left(\frac{3b^3\Delta\gamma}{akT}\right)^2 \frac{1}{\Delta\chi} \tag{8}$$

where $\Delta\chi = \chi_b - \chi_{S/VME}$. In eq 8, b^3, the volume of a Flory–Huggins lattice site, is deduced for PS as 1.41×10^{-28} m^3 and PVME as 0.787×10^{-28} m^3 from the hard-core specific volumes.[6] For the blends, b^3 is the volume fraction average. The surface energy difference, $\Delta\gamma$, is known to be 0.008 J/m^2.[6] The parameter a, the effective step length defined by the mean end-to-end distance, turned out to be 7.0×10^{-10} m, which is the same for both PS and PVME.[6] The parameter χ_b, introduced by Jones and Kramer,[17] as the interaction parameter on the coexistence curve, and thus the critical interaction parameter, is defined by eq 9.

$$\chi_b = \frac{1}{N(1 - 2C_b)} \ln\left(\frac{1 - C_b}{C_b}\right) \tag{9}$$

where N is the degree of polymerization. Cowie tested this theory with their IR-ATR obtained results,[6] assuming χ to be zero. In their case, C_s for PVME was unity for all values of C_b. However, Kwei et al. found that the experimental χ values depend on the composition and ranged from −0.75 to −0.17 in the miscible range of 35–65 wt %.[30]

With the known densities of PS and PVME, the surface weight fraction C_s was estimated and plotted in Figure 4 as open triangles, for comparison. The predicted PVME contents from 40% to 60% blends are close to the experimental data, even though the theory may represent more surface-sensitive composition.

Comparison of UV Reflectance Results with ESCA Results. For quantitative analysis of PS/PVME blends, C_{1s} spectra are generally used. The C_{1s} spectra for pure PVME shows two peaks containing contributions from carbon–oxygen (at 286.6 eV) and carbon–hydrogen bonds (at 285 eV). On the other hand, the C_{1s} spectra for PS show only one carbon–hydrogen peak. Therefore, surface composition can be calculated from these spectra by resolving the two contributions and calculating the integrated area under each peak.

The area intensity ratio of hydrogen carbon to oxygen carbon is equal to the average atomic ratio of the two types of carbon atoms and is given by[1]

$$\frac{I_{CH}}{I_{CO}} = \left(\frac{C_s}{M_{PVME}} + \frac{8(1 - C_s)}{M_{PS}}\right) \Big/ \frac{2C_s}{M_{PVME}} \tag{10}$$

where C_s is the average weight fraction of PVME within the sampling depth. M_{PS} and M_{PVME} are the molecular weights of the styrene and vinyl methyl ether repeat units, respectively.

The PVME content at the surface, solved from eq 10, can be expressed as

$$C_s = \frac{1}{1 + (1/8)(M_{PS}/M_{PVME})\{2(I_{CH}/I_{CO}) - 1\}} \tag{11}$$

The ESCA results of quantitative analysis for the PS/PVME blends (80/20, 60/40, and 40/60) were obtained and corrected by dividing the value, $(1 + x)$ where x is the extent of hydrocarbon contamination[1] measured on pure PVME films.

The ESCA results were compared with the UV results, as illustrated in Figure 5 as filled triangles. From Figure 5, we can see that the surface enrichment of PVME in ESCA data is more significant than in UV reflection data, indicating greater PVME concentration and concentration gradient as one measures very close to the surface.

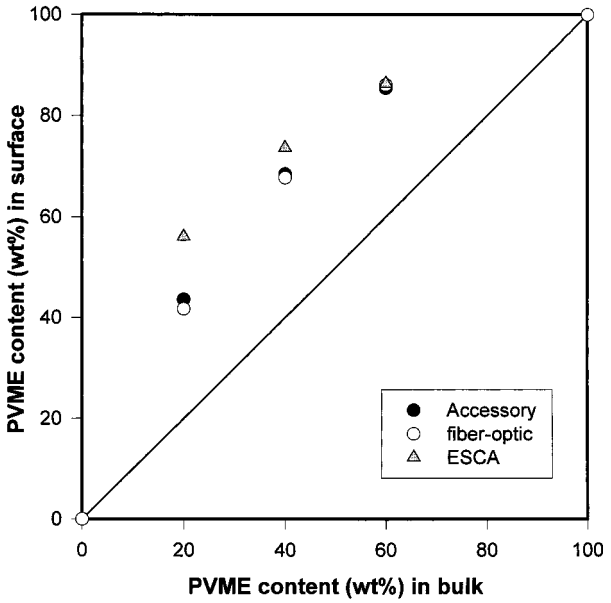

Figure 5. Comparison of PS/PVME results by using bifurcated optical-fiber attachment and ESCA.

In Situ Surface Composition Analysis. To develop in-situ surface composition analysis technique, UV reflection attachment using bifurcated optical fiber as shown in Figure 1b was tested in PS/PVME blends. UV reflection spectra of PS/PVME blends via fiber-optic attachment are very similar to those when the reflection accessory is used. After Kramers–Kronig conversion of the reflection spectra, the surface compositions obtained by fiber-optic attachment are very close to the results obtained by reflection accessory as illustrated in Figure 5 as open circles.

This result demonstrates that it is possible to measure the surface composition directly by UV reflection in-situ, in cases where sampling is inconvenient such as when the film is on metal surfaces.

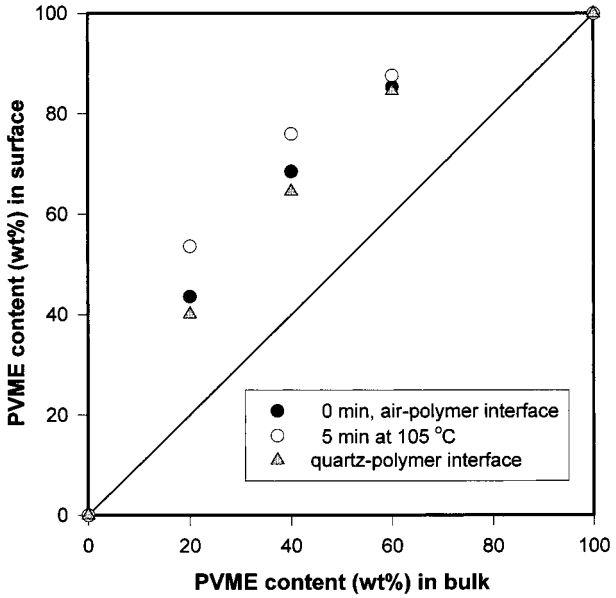

Figure 6. Comparison of PS/PVME results with substrate effect and annealing effect, using reflection accessory.

Substrate and Annealing Effect. It is known that the surface composition on the substrate facing side is often different from the bulk composition depending on the surface properties of substrates.[2] In our studies, it is possible to analyze the surface composition on the quartz side without disturbing the film, due to the transparency of quartz to UV light. The reflection spectra of PS from quartz side is very similar to those from the air side, since the reflection spectra of quartz is very flat until 185 nm. The surface composition on quartz side is thus obtained from Kramers−Kronig transformation of UV reflection spectra and compared with the air facing side results in Figure 6 as filled triangles. The results show the enrichment of PVME on quartz side, but to a slightly less extent than the air side. This enrichment of PVME on quartz side may be attributed to a preferential adsorption of PVME segments to the hydrophilic quartz surface to minimize the polymer−quartz interfacial energy.

It has been reported that the heat treatment on miscible PS/PVME blends can induce phase separation and greater enrichment of PVME on the air-facing surface.[31−33] To test whether UV reflection results can confirm such a trend, we annealed the miscible blends at 105 °C, which is above its lower critical solution temperature (LCST),[31] for 5 min in a convection oven. The results are shown in Figure 6 as open circles, in comparison to the composition before annealing. It is clear that annealing leads to greater PVME enrichment, especially with 20 wt % and 40 wt % PVME blends, thus confirming the trend observed by the work of Pan and Prest,[33] who annealed the blends at 154 °C for 10 min.

Summary

In miscible blends of PS/PVME, the surface chemical compositions of PVME were estimated from UV reflection spectra and Kramers−Kronig transformation, probing the surface depth of a few hundred angstroms. Results showed that the surface of PS/PVME blend is significantly enriched with PVME, the component with the lower surface energy. The experimental results were compared with the predictions from the simplified mean-field theory, and good agreement was found. In addition to UV reflection, ESCA data were obtained to measure the surface chemical composition of PS/PVME blends. The surface enrichment of PVME in ESCA data were more significant than in UV reflection data for all compositions of the blends tested, suggesting a concentration gradient. ESCA and UV reflection for characterization of surface chemical composition provide the information for different probing depth, and therefore UV reflection can be used as another tool to investigate the range that ESCA cannot approach.

The surface compositions obtained by bifurcated optical-fiber attachment were very close to the result obtained by reflection accessory, thus showing the promise of the UV remote sensing technique for in-situ surface composition analysis without sampling. The polymer−quartz interface showed enrichment of PVME, probably due to preferential adsorption of PVME to hydrophilic surface of synthetic quartz, but its extent was less than the air−polymer interface. The surface enrichment effect was more pronounced in thermally treated blends produced by heating above the LCST, consistent with a previously reported trend.

Acknowledgment. Thanks are due to Ms. D. A. Smith at the Institute of Material Science for her help in performing ESCA experiments. We are also indebted to N. J. Kim and M. D. Weir for valuable discussion.

References and Notes

(1) Batia, Q. S.; Pan, D. H.; Koberstein, J. T. *Macromolecules* **1988**, *21*, 2166.
(2) Tanaka, K.; Takahara, A.; Kajiyama, T. *Macromolecules* **1996**, *29*, 3232.
(3) Tanaka, K.; Yoon, J. S.; Takahara, A.; Kajiyama, T. *Macromolecules* **1995**, *28*, 934.
(4) Tanaka, K.; Takahara, A.; Kajiyama, T. *Macromolecules* **1998**, *31*, 863.
(5) Hong, P. P.; Boerio, F. J.; Smith, S. D. *Macromolecules* **1994**, *27*, 596.
(6) Cowie, J. M. G.; Devlin, B. G.; McEwen, I. J. *Macromolecules* **1993**, *26*, 5628.
(7) Affrossman, S.; O'Neil, S. A.; Stamm, M. *Macromolecules* **1998**, *31*, 6280.
(8) Cowie, J. M. G.; Devlin, B. G.; McEwen, I. J. *Macromolecules* **1993**, *26*, 501.
(9) Clark, M. B., Jr.; Burkhardt, C. A.; Gardella, J. A., Jr. *Macromolecules* **1989**, *22*, 4495.
(10) Zhao, X.; Sokolov, J.; Rafailovich, M. H.; Schwarz, S. A.; Wilkens, B. J.; Jones, R. A.; Kramer, E. J. *Macromolecules* **1991**, *24*, 5991.
(11) Norton, L. J.; Kramer, E. J.; Bates, F. S.; Gehlsen, M. D.; Jones, R. A. L.; Karim, A.; Felcher, G. P.; Kleb, R. *Macromolecules* **1995**, *28*, 8621.
(12) Li, L.; Sosnowski, S.; Chaffey, C. E.; Balke, S. T.; Winnik, M. A. *Langmuir* **1994**, *10*, 2495.
(13) Kaito, A.; Nakayama, K.; Kanetsuna, H. *J. Polym. Sci., Part B: Polym. Phys.* **1988**, *26*, 1439.
(14) Kaito, A.; Nakayama, K.; Kyotani, M. *J. Polym. Sci., Part B: Polym. Phys.* **1991**, *29*, 1321.
(15) (a) Paik, H. J.; Hestermann, D. K.; Sung, N. H. *SPE Proc.* **1995**, 2816. (b) Yu, J. W.; Sung, C. S. P. *Macromolecules* **1995**, *28*, 2506.
(16) Jones, R. A. L.; Kramer, E. J. *Polymer* **1993**, *34*, 115.
(17) Hestermann, D. K.; Sung, N. H. *PMSE Proc.* **1996**, *75*, 387.
(18) Patridge, R. H. *J. Chem. Phys.* **1967**, *47*, 4223.
(19) Carter, J. G.; Jelinek, T. M.; Hamm, R. N.; Birkhoff, R. D. *J. Chem. Phys.* **1966**, *44*, 2266.
(20) Hansen, W. N. *Spectrochim. Acta* **1965**, *21*, 815.
(21) In this work we assumed normal incident angle because the reflectance is quite weakly dependent on the angle of incidence at small angle (6°).
(22) Jahoda, F. C. *Phys. Rev.* **1957**, *107*, 1261.
(23) Bortz, M. L.; French, R. H. *Appl. Spectrosc.* **1989**, *43*, 1498.

(24) Ohta, K.; Ishida, H. *Appl. Spectrosc.* **1988**, *42*, 952.
(25) See, for example, a software from Galactic Industries Corp.
(26) Hornbeck, R. W. *Numerical Methods;* Prentice Hall: W. Nyack, NY, 1975.
(27) Carnahan, B. *Applied Numerical Methods*; Krieger Publishing: Melbourne, FL, 1990.
(28) (a) Roessler, D. M. *Br. J. Appl. Phys.* **1965**, *16*, 1119. (b) Roessler, D. M. *Br. J. Appl. Phys.* **1966**, *17*, 1313.
(29) Nishi, T.; Kwei, T. K. *Polymer* **1975**, *16*, 285.
(30) Kwei, T. K.; Nishi, T.; Roberts, R. F. *Macromolecules* **1974**, *7*, 667.
(31) Bank, M.; Leffingwell, J.; Thies, C. *J. Poym. Sci., Part A-2* **1972**, *10*, 1097.
(32) Nishi, T.; Wang, T. T.; Kwei, T. K. *Macromolecules* **1975**, *8*, 227.
(33) Pan, D. H. K.; Prest, W. M., Jr. *J. Appl. Phys.* **1985**, *58*, 2861.

MA000633Y